

## In-situ cosmogenic $^{14}\text{C}$ analysis at ETH Zürich: Characterization and performance of a new extraction system



Maarten Lupker<sup>a,\*</sup>, Kristina Hippe<sup>b,c</sup>, Lukas Wacker<sup>b</sup>, Olivia Steinemann<sup>b</sup>, Dmitry Tikhomirov<sup>b,d</sup>, Colin Maden<sup>e</sup>, Negar Haghypour<sup>a</sup>, Hans-Arno Synal<sup>b</sup>

<sup>a</sup> Geological Institute, ETH Zürich, Switzerland

<sup>b</sup> Ion Beam Physics, ETH Zürich, Switzerland

<sup>c</sup> Institute of Geological Sciences, Freie Universität, Berlin, Germany

<sup>d</sup> Department of Geography, University of Zürich, Switzerland

<sup>e</sup> Institute of Geochemistry and Petrology, ETH Zürich, Switzerland

### ARTICLE INFO

#### Keywords:

In-situ  $^{14}\text{C}$

Cosmogenic nuclide

Methods

### ABSTRACT

We present a new in-situ cosmogenic  $^{14}\text{C}$  extraction system developed at ETH Zürich. This system quantitatively extracts  $^{14}\text{C}$  produced in quartz by cosmic rays using a high temperature extraction procedure. A key improvement of the new extraction system is the implementation of largely automated sequences,  $\text{CO}_2$  transport in a He flow and the addition of a “dead”  $\text{CO}_2$  carrier gas, which ensure highly reproducible operation while limiting the required operator attendance. Intercomparison quartz samples were routinely measured over a year of operation and yield  $^{14}\text{C}$  concentrations of  $7.27 (\pm 0.03) \cdot 10^5$  at/g quartz for CRONUS-A ( $n = 7$ ) and  $1.24 (\pm 0.17) \cdot 10^4$  at/g quartz for CRONUS-N ( $n = 4$ ). The excellent performance of the new system is highlighted by low procedural blanks of ca.  $3 \cdot 10^4$   $^{14}\text{C}$  atoms and coefficients of variation for the CRONUS-A and CRONUS-N analyses of only 0.4% and 14% respectively.

### 1. Introduction

Cosmogenic nuclides are produced at the Earth surface through the interaction between cosmic rays and target atoms in rock minerals [21]. Nuclides such as  $^{10}\text{Be}$ ,  $^{26}\text{Al}$ ,  $^{36}\text{Cl}$ ,  $^3\text{He}$  and  $^{21}\text{Ne}$  are frequently used to constrain exposure durations of geomorphic objects or denudation rates over a wide range of temporal and spatial scales [2]. Cosmogenic  $^{14}\text{C}$  produced within quartz – hereafter termed in-situ  $^{14}\text{C}$  – is a relatively recent addition to the terrestrial cosmogenic nuclide toolbox [24] and it opens new opportunities in Earth surface processes and terrestrial paleoclimate studies [12]. The 5700 yr half-life of  $^{14}\text{C}$  (National Nuclear Data Center, B.N.L., [www.nndc.bnl.gov](http://www.nndc.bnl.gov)), much shorter than of other nuclides (e.g.,  $^{10}\text{Be}$  with 1.4 Myr), makes it suitable to study surface processes over post-LGM to Holocene time scales.

The range of applications of in-situ  $^{14}\text{C}$  is expanding as an increasing number of extraction systems become available. In-situ  $^{14}\text{C}$  has proven useful in combination with  $^{10}\text{Be}$  to disentangle complex surface exposure histories that cannot be resolved using a single nuclide. Applications so far include complex glacier chronologies and subglacial erosion, the detection of recent landscape transience and erosion events as well as the quantification of sediment residence times in different

geomorphic systems [26,1,32,10,9,16,13,20,19,3,4,33,27]. The fast decay of  $^{14}\text{C}$  makes it sensitive to short-term episode of exposure or burial but insensitive to nuclide inheritance that may for instance affect the long-lived  $^{10}\text{Be}$ . In parallel to the emergence of new applications, efforts have been undertaken to increase the accuracy of dates and rates obtained using in-situ  $^{14}\text{C}$  through improved calibration of the in-situ  $^{14}\text{C}$  production rate [28,34,25,22].

Due to the growing interest in a more systematic application of in-situ  $^{14}\text{C}$  analysis to Earth surface process questions, new analytical developments have recently been made to simplify and streamline in-situ  $^{14}\text{C}$  measurements [15,11,8,23,6,4,5,7]. The measurement of in-situ  $^{14}\text{C}$  concentrations nevertheless remains analytically challenging because of the need to remove atmospherically derived  $^{14}\text{C}$  adsorbed to quartz grain surfaces and the overall small amounts of in-situ produced  $^{14}\text{C}$  that are present in quartz. This has led to the development of a number of different designs in in-situ  $^{14}\text{C}$  extractions systems. All these systems have the same objective of quantitatively releasing carbon from the quartz crystal lattice at high temperatures, converting it to  $\text{CO}_2$  and purifying the  $\text{CO}_2$  from other trace gases. The total amount of captured  $\text{CO}_2$  is then measured prior to the analysis of its  $^{14}\text{C}/^{12}\text{C}$  (or  $^{14}\text{C}/^{13}\text{C}$ ) ratio by accelerator mass spectrometry (AMS) with or without prior

\* Corresponding author.

E-mail address: [maarten.lupker@erdw.ethz.ch](mailto:maarten.lupker@erdw.ethz.ch) (M. Lupker).

<https://doi.org/10.1016/j.nimb.2019.07.028>

Received 12 March 2019; Received in revised form 12 July 2019; Accepted 22 July 2019

Available online 25 July 2019

0168-583X/ © 2019 The Author(s). Published by Elsevier B.V. This is an open access article under the CC BY-NC-ND license

(<http://creativecommons.org/licenses/by-nc-nd/4.0/>).

graphitization [12].

Until recently, in-situ  $^{14}\text{C}$  extraction at ETH Zürich was performed using a high vacuum extraction system that innovated with the use of all-metal tubing (as opposed to glass) and a high temperature furnace that avoided the use of a melting flux during the extraction [14,33]. This design has been routinely used since 2009 and contributed in-situ  $^{14}\text{C}$  data for various studies in sedimentary and glacial environments [16,3,20,19,3,25,33]. However, to overcome long maintenance procedures, to increase sample throughput and to improve data reproducibility a new extraction system was constructed and tested over the past two years. This contribution is aimed at communicating the recent advances made at ETH Zürich with the development of this new in-situ  $^{14}\text{C}$  extraction system and to share its characteristics and performance.

## 2. Extraction system description

### 2.1. Set-up

The new ETH in-situ  $^{14}\text{C}$  extraction system can be schematically divided into three parts: i) the furnace for  $^{14}\text{C}$  extraction, ii) the low vacuum part for automated gas cleaning, and iii) the high vacuum part for manual gas cleaning (Fig. 1).

The furnace setup consists of a sapphire tube (Crytur, 22.7 mm ID, 570 mm long), which is closed on one end and held horizontally in a high temperature resistance furnace (Carbolite Gero, HTRH18/40/250). The open end of the sapphire tube extends beyond the furnace and connects to a stainless steel (SS) flange with 3 Viton O-rings. The flange and the open end of the sapphire tube are water-cooled in between the two O-rings closest to the furnace. The sapphire tube and flange are closed by a DN40 all-metal gate valve (VAT) that allows for simple sample loading and exchange. The pressure in the sapphire tube is continuously monitored by with a piezo pressure transducer (MKS, 902B) connected to the controlling computer.

The extraction furnace connects to the low vacuum part via 1/16" SS tubing and pneumatically actuated valves (VICI ASFVOL & ASFVL). The valve and tubing setup allows filling, flushing and exchange of different gases in the sapphire tube and the attached metal tubing throughout the entire low vacuum part. The system utilizes three external gas supplies: He (4.6 grade or 99.996% purity) as a transport gas, a  $\text{O}_2$ -He mixture (1:9 vol, 4.6 purity) for quartz cleaning and  $^{14}\text{C}$  extraction, and a  $\text{CO}_2$ -He mixture (2:8 vol, PanGas – The Linde Group) as carrier gas. The  $\text{O}_2$ -He and  $\text{CO}_2$ -He cylinders connect to a 6-port valve (VICI, AC6WE) which is equipped with a sample loop (Fig. 1). This configuration allows sampling and injection of a fixed amount of  $\text{CO}_2$ -He carrier into the sapphire tube. The rest of the low-vacuum part is designed to clean and trap the  $\text{CO}_2$  sample after release from the extraction furnace and to transport the sample to the high vacuum part. The primary gas cleaning steps involve passage through a quartz tube filled with cut copper (Cu) wire and silver (Ag) wool followed by a chemical water trap filled with phosphorus pentoxide. The Cu-Ag tube is maintained at 550 °C by a resistance furnace (Carbolite Gero, MTF 12/25/250) to remove halogenes and sulfur compounds (Fig. 1). Downstream, the water trap is attached through an in-line 0.5  $\mu\text{m}$  filter (Swagelok, SS-4FWS-VCR-05) to a cryogenic sample trap. The cold trap is made of several loops of 1/4" SS tubing bracketed by pneumatic valves on both ends (Swagelok, SS-BNV51-C) and liquid nitrogen (LN) is added manually. The current line design does not include any flow of the extracted gases over a high-temperature furnace filled with Qz-beads as is the case with other setups to ensure possible CO is converted to  $\text{CO}_2$ . As shown further down, high  $\text{CO}_2$  yields and  $^{14}\text{C}$  concentrations in the same range, or above, other systems do not suggest any significant incomplete CO conversion. All gases are evacuated by a scroll roughing pump (Edwards, NXD6i), either directly via a connection close to the sapphire tube or through a second connection further downstream that forces the gases to pass the Cu-Ag tube and chemical water trap. During standby mode, the low vacuum part is continuously flushed with

helium to maintain a low  $^{14}\text{C}$  background. The helium flow rate of 10  $\text{ml}_n/\text{min}$  is regulated by a flowmeter (Voigtlin, GCR). The furnace and connected tubing are operated at a typical pressure range of 10–500 mbar, which provides efficient transport of the extracted gases within a laminar flow regime.

Apart from the pneumatic valves, the pressure in the sapphire tube and furnace temperature are computer-controlled using a dedicated program written in LabVIEW. The pneumatic valves are controlled through a digital I<sup>2</sup>C interface and a solenoid valve rack (Ionplus) fed by a central pressurized air supply of the building. The pressure sensor of the sapphire tube and a temperature controller of the extraction furnace are controlled through RS232/485 interfaces. The control software was written to automate most of the gas handling steps during the extraction except for the last gas cleaning steps in the high vacuum part of the line, which are done manually.

The high vacuum part of the line is assembled of Swagelok VCR connectors and manual membrane valves (Swagelok, SS-4H-V51). From upstream to downstream, this part consists of a cryogenic cold finger equipped with a Pirani pressure sensor (Pfeiffer, TPR280), a calibrated volume equipped with a high-precision pressure transducer (MKS, Baratron 626C12TBE) and a glass tube (4 mm OD) which is used to collect and seal the purified  $\text{CO}_2$  sample. Vacuum in this part of the line is maintained by a turbomolecular membrane pump pumping unit (Pfeiffer, HiCube 80) and monitored with a Pirani - cold cathode combined pressure sensor (Pfeiffer, PKR 251). Great care was taken to minimize overall volume of the high vacuum part and keep a straight gas path in the line of sight of the turbomolecular pump to ensure efficient and fast pumping. Typically attained pressures are ca.  $1 \cdot 10^{-8}$  mbar.

A critical component for the accuracy of the in-situ  $^{14}\text{C}$  measurement is an accurate determination of the amount of  $\text{CO}_2$  extracted from a given sample. The new extraction line relies on measurement of the gas pressure in a cold finger of exactly known volume. The volume of the pre-assembled setup of cold finger including valves and pressure transducer was measured with a dedicated calibration line in the ETH Zürich Noble Gas laboratory [30]. The cold finger setup was maintained at constant temperature in a water bath and filled with nitrogen ( $\text{N}_2$ ) using a calibration pipette with a relative volume uncertainty of less than 1‰, while the pressure difference was monitored. The procedure was repeated 8 times and averaged, yielding a final calibrated volume for the cold finger setup of  $14.460 (\pm 0.015) \text{ cm}^3$ .

### 2.2. Extraction procedure and gas cleaning

The extraction and gas cleaning procedures resemble those previously established at ETH [14,15]. A purified quartz sample (100–1000  $\mu\text{m}$  grain-size) is treated with ca. 30% nitric acid ( $\text{HNO}_3$ ) for at least one hour at 80 °C and in an ultrasonic bath. After drying, about 3–6 g of precleaned quartz is precisely weighed into a platinum (Pt) boat (10 × 10 × 50 mm). The quartz-filled Pt-boat is slid into the sapphire tube on a small sapphire pad (ca. 10 × 100 mm), which is used to prevent the Pt-boat to directly stick to the sapphire tube. Except during sample loading, cleaning and extraction procedures, the sapphire tube is maintained filled with He gas at ca. atmospheric pressure.

After the gate valve is closed, the line operator starts an automated sample cleaning and extraction procedure, which executes the following steps (Fig. 2):

- The sapphire tube is evacuated from atmospheric pressure to 50 mbar, filled again to 500 mbar with He and evacuated to 50 mbar. The filling-evacuation cycle is repeated twice before the sapphire tube is evacuated to 10 mbar. Subsequently, all other tubing of the low vacuum part of the line is flushed five times with He.
- The first heating step is performed to remove all adsorbed atmospheric  $\text{CO}_2$  from the quartz surface. This is achieved by heating the

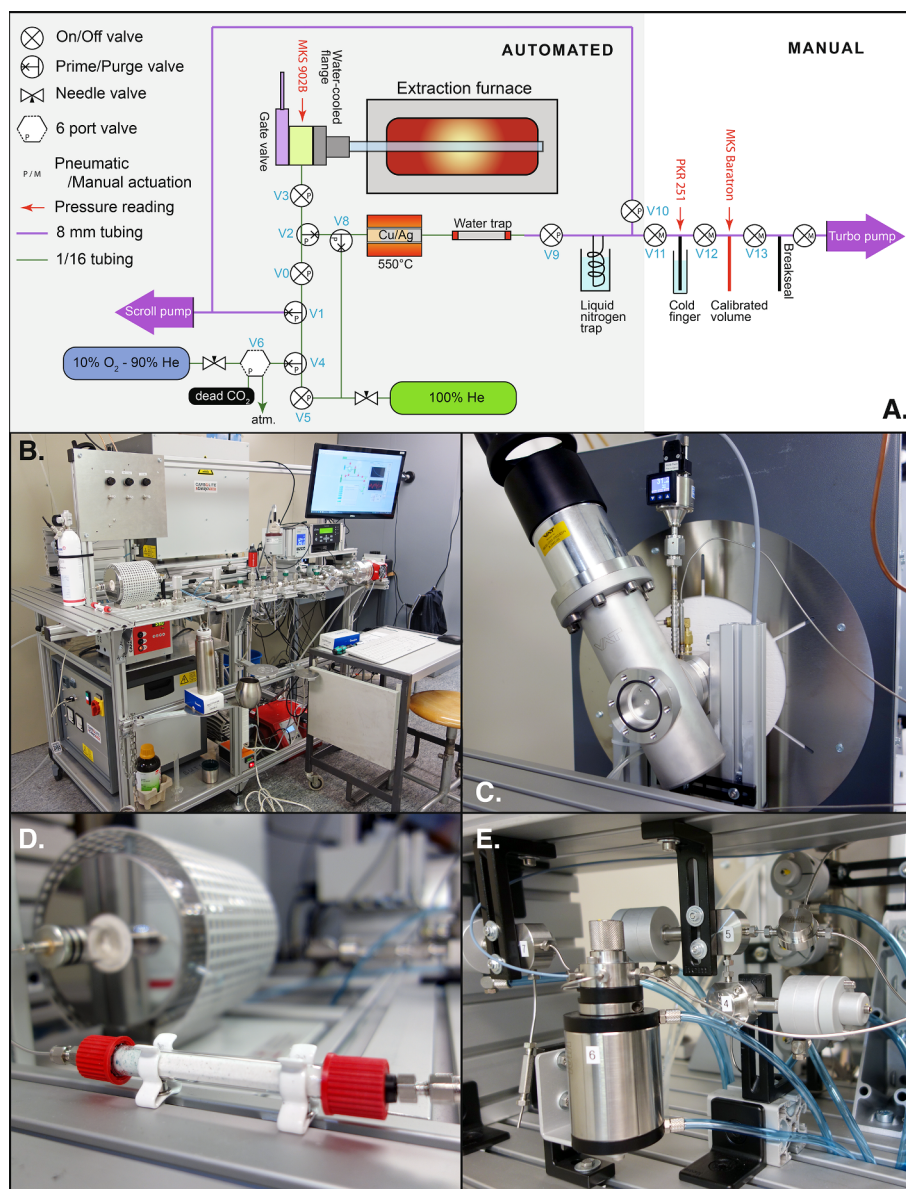


**Fig. 1.** A. Sketch of the in-situ  $^{14}\text{C}$  extraction line. B. General overview of the line during normal operation. C. Gate valve and water-cooled flange connecting to the sapphire tube holding the sample during extraction. D. Chemical water trap used to remove  $\text{H}_2\text{O}$  produced during extraction (Cu-Ag-filled quartz tube in the furnace in the background). E. Pneumatic valves controlling the gas handling ( $\text{He}$  &  $\text{He-O}_2$ ) during the cleaning and extraction steps.

sample to  $500\text{ }^\circ\text{C}$  (ramp of  $10\text{ }^\circ\text{C}/\text{min}$ ) and maintaining this temperature for 2 h. During this step, the sapphire tube is filled with  $500\text{ mbar He-O}_2$  and evacuated to  $50\text{ mbar}$  for a total of 8 times (ca. 20 min per cycle including heating up).

- Following the first heating step, a fixed amount of  $\text{CO}_2$  carrier gas (ca.  $17\text{ }\mu\text{g}$ ) is sampled using the injection loop and flushed into the sapphire tube with a flow of  $\text{O}_2\text{-He}$  mixture until a pressure of ca.  $200\text{ mbar}$  is attained. At this point, the sapphire tube is isolated and the furnace is heated up to  $1670\text{ }^\circ\text{C}$  ( $10\text{ }^\circ\text{C}/\text{min}$ ), a temperature that is maintained for 3 h. The  $\text{O}_2\text{-He}$  mixture ensures an excess of  $\text{O}_2$  to transform all released carbon compounds into  $\text{CO}_2$ . The amount of  $\text{CO}_2$  carrier gas injected for an extraction is estimated based on the total amount of  $\text{CO}_2$  measured after all blank extractions. Because the system relies on the calibrated volume setup, the exact pressure and volume of the injection loop is unknown and not needed.
- After the 3 h of extraction, the furnace temperature is slowly decreased ( $5\text{ }^\circ\text{C}/\text{min}$ ). At a temperature of  $1550\text{ }^\circ\text{C}$ , the operator can start cleaning of the extracted gases. The sample gases are pumped

through the Cu-Ag furnace, the chemical water trap and finally through the cryogenic trap, where  $\text{CO}_2$  freezes at LN temperature ( $-196\text{ }^\circ\text{C}$ ). These cleaning steps ensure removal of significant amounts of excess  $\text{O}_2$ ,  $\text{NO}_x$  and water produced during extraction. Once the pressure in the sapphire tube drops from  $200\text{ mbar}$  to  $50\text{ mbar}$ , three sequences of He-flushing (filling to  $500\text{ mbar}$ , evacuation to  $50\text{ mbar}$ , see Fig. 2) are performed to ensure collection over 99.9% of the  $\text{CO}_2$  sample in the cryogenic trap. Tests with 4 to 5 He-Flushing sequences did not result in higher  $\text{CO}_2$  recovery suggesting that all  $\text{CO}_2$  is effectively collected. The Cu-Ag is reduced with  $\text{H}_2$  and the phosphorus pentoxide of the water trap is replaced every ca. 50 extractions.

After these initial automated steps, the final gas cleaning is done manually. However, the cleaning sequence is timed and instructions are given by the control program to ensure a high reproducibility of the sample extraction. Each transfer of the sample gas is immediately followed by closing of the adjacent upstream valve to avoid backstreaming

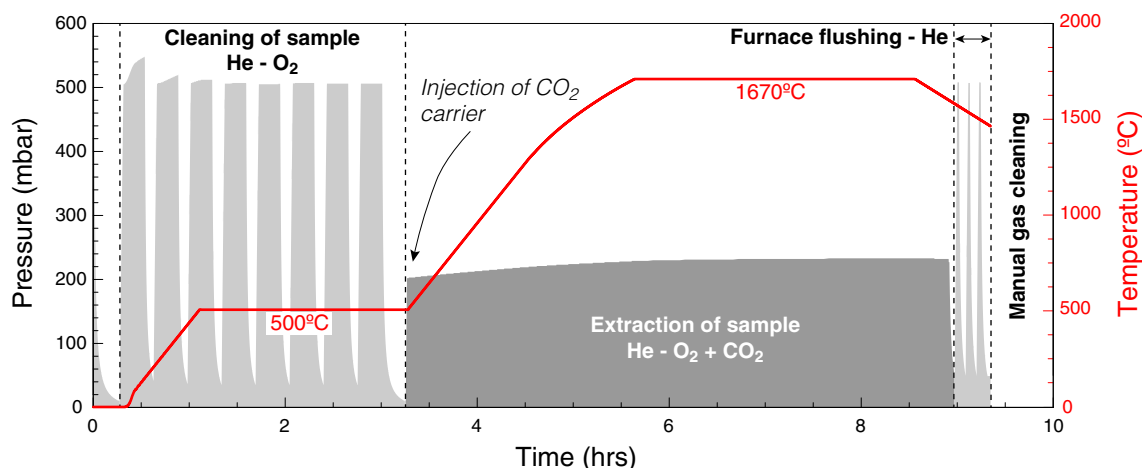


Fig. 2. Overview of the complete operational sequence, with gas pressures in the furnace shown in different shades of grey and furnace temperature in red. The quartz sample is loaded at  $t = 0$  h and the clean  $\text{CO}_2$  gas can be collected in a glass tube for AMS analysis at  $t = 10$  h.

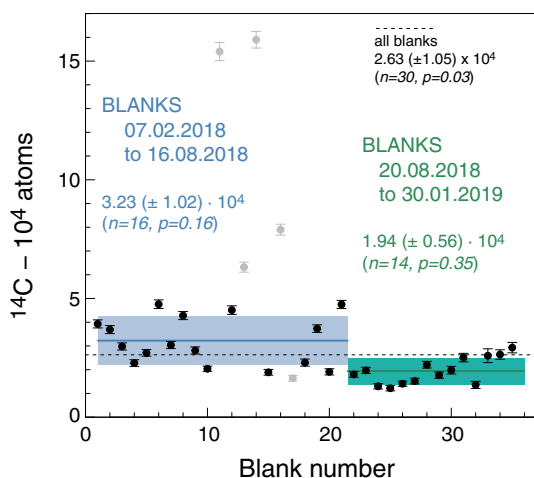


Fig. 3. Procedural blanks ( $\pm 1\sigma$ ) measured on the new ETH extraction system. Blanks were split into two normally-distributed groups from 07.02.2018 to 16.08.2018 and from 20.08.2018 to 30.01.2019 suggesting an improvement in overall blank level over time. These average blanks values were used to correct all measurements made during the two respective periods. Measurement after maintenance were not considered and are indicated in light grey.

of the  $\text{CO}_2$ . The sample with remaining other gases are first released from the cryogenic trap and frozen in the adjacent cold finger using LN. Gases are released again from the cold finger by heating it to room temperature followed by cooling down to  $-145^\circ\text{C}$  for 15 min using a variable temperature trap (VTT) (see [14] for details on the VTT). At this temperature the  $\text{CO}_2$  remains in the gas phase while contaminant gases such as  $\text{SO}_2$  or remaining water are trapped in the VTT. The  $\text{CO}_2$  is transferred from the cold finger to the calibrated volume with LN while the cold finger is maintained at  $-145^\circ\text{C}$ .  $\text{CO}_2$  is then released in the calibrated volume and left to equilibrate with ambient temperature. Pressure and temperature of the calibrated volume are recorded to calculate the total amount of  $\text{CO}_2$  following the ideal gas law. Finally, the sample is transferred and trapped with LN into the glass breakseal tube, which is sealed with a hand torch and ready for AMS measurement.

The duration of an extraction from loading of the quartz sample to sealing of the glass breakseal is ca. 10 h, most of which is automated (Fig. 2). After sample extraction and cooling down of the furnace, the Pt-boat is restored by treatment with hydrofluoric acid ( $\text{HF} - 48\%$ ) and  $\text{HNO}_3$  (65%) (9  $\text{HF}:1 \text{HNO}_3$  vol.) to remove all quartz. The empty boat is re-used after proper degassing going through a complete extraction

procedure without quartz. Therefore, during routine operation, the extraction system is used to extract a sample over a day, preceded by the sample boat cleaning on the day before.

### 3. Results and discussion

Measurements of the  $^{14}\text{C}/^{12}\text{C}$  ratio were done on ETH MICADAS 200 kV AMS instrument equipped with a gas ion source, which does not require graphitization of the samples [29]. The purified  $\text{CO}_2$  collected in sealed glass tubes is transferred into an automatic cracker system and the sample is flushed with He directly into the AMS ion source [31]. The measured  $^{14}\text{C}/^{12}\text{C}$  ratios were converted to absolute  $^{14}\text{C}$  concentrations following Hippe and Lifton [17]. All data is provided in the Electronic Appendix Table.

#### 3.1. Blanks

The procedural blank is determined applying the same extraction procedure as described above, but using an empty Pt-boat. Blanks are usually measured every 4–6 samples during normal line operation. Additional blanks are run after maintenances or longer periods of inactivity. Over the last ca. 1 year of operation 35 procedural blanks were measured, five of which are outliers as they were run during system testing or after maintenance, or because of obvious system malfunction. The long-term procedural blank at the time of writing (March 2019) is  $2.63 (\pm 1.05) \cdot 10^4$  atoms  $^{14}\text{C}$  ( $n = 30$ ) using a 1 standard deviation around the mean uncertainty estimate (Fig. 3) but the distribution is not well fitted by a normal distribution ( $p = 0.03$ ). However, the blank data can be sub-divided into two, normally-distributed, populations with mean blank values of  $3.23 (\pm 1.02) \cdot 10^4$  atoms  $^{14}\text{C}$  ( $n = 16$ ,  $p = 0.16$ ) and  $1.94 (\pm 0.56) \cdot 10^4$  atoms  $^{14}\text{C}$  ( $n = 14$ ,  $p = 0.35$ ) for the periods from 07.02.2018 to 16.08.2018 and from 20.08.2018 to 30.01.2019 respectively. The improvement in blank levels between these two periods could not be traced back to a specific maintenance operation and could therefore reflect a more general blank improvement over time. Samples and standards were corrected based on their extraction date and the respective blank level estimate of the corresponding period.

The total amount of  $\text{CO}_2$  gas collected for a typical blank is  $17.4 (\pm 0.6)$  gC and represents the combination of the injected “dead”  $\text{CO}_2$  carrier gas and the  $\text{CO}_2$  contamination of the system during the extraction.

The blank level determined for the new system is in the same range, though slightly lower compared to the average  $3.48 (\pm 2.05) \cdot 10^4$  atoms  $^{14}\text{C}$  ( $n = 45$ ) long-term blank measured on the previous extraction line at ETHZ [25]. As with other systems [22,25], it

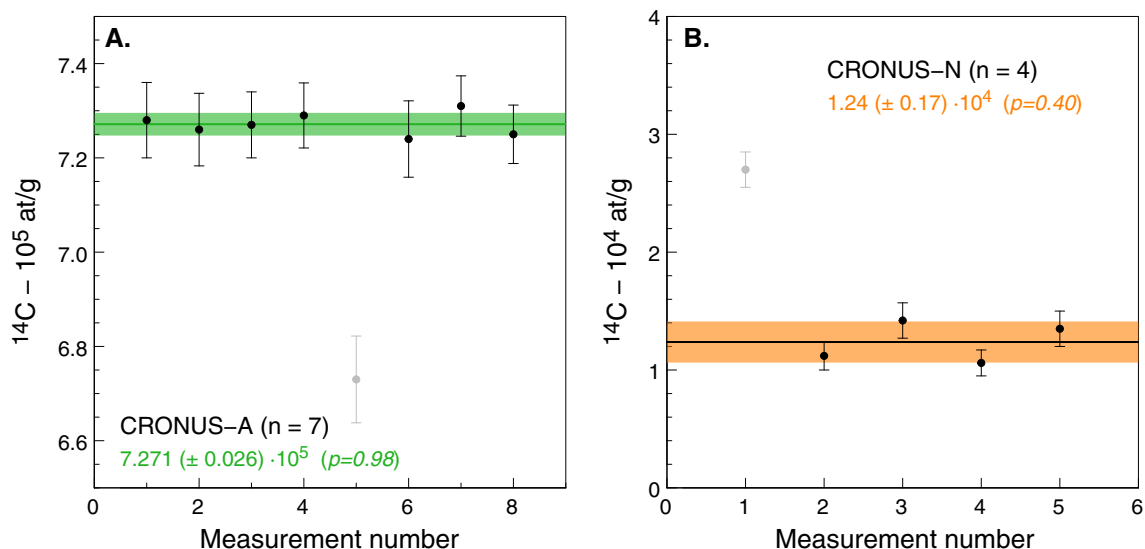


**Fig. 4.** Measured concentration of the quartz intercomparison materials CRONUS-A (A.) and CRONUS-N (B.) with  $\pm 1\sigma$  measurement uncertainty (comprising uncertainties for the AMS measurement and blank subtraction). Mean  $^{14}\text{C}$  concentrations are also given with  $\pm 1$  standard deviation (green/orange band). One CRONUS-A and one CRONUS-N measurement were considered an outlier (grey) and not included in the reported statistics even though no anomaly was recorded during the extraction.

was found that continuous, nearly uninterrupted operation of the extraction line tends to keep blank levels low. There is a clear reduction in blank variance for the new system (40% for the all valid blank measurements instead of 59% previously), which we attribute to the use of a  $\text{CO}_2$  carrier. Addition of a carrier gas minimizes the impact of possible losses of small amounts of gas during extraction and cleaning because overall larger amounts of  $\text{CO}_2$  are transferred through the line.

### 3.2. Reproducibility

Two quartz samples distributed as reference materials for interlaboratory comparison were measured to check yields and performance of the new  $^{14}\text{C}$  extraction system: CRONUS-A, a high concentration quartz from exposed sandstone outcrops in Antarctica and CRONUS-N, a low concentration quartz from beach sand in Australia. Both quartz materials have been previously analyzed by a number of labs for  $^{10}\text{Be}$ ,  $^{26}\text{Al}$  and in-situ  $^{14}\text{C}$ , including in-situ  $^{14}\text{C}$  analyses at the previous extraction system at ETHZ [18]. Recent publications have reported additional  $^{14}\text{C}$  data for CRONUS-A and -N [11,8,22,4,5].

CRONUS-A was measured eight times in 2018. Measured concentrations were corrected for a normally distributed blank value of  $3.23 (\pm 1.02) \cdot 10^4$  atoms for the first seven measurements and  $1.94 (\pm 0.56) \cdot 10^4$  atoms for the last one (Fig. 4). The blank represents less than ca. 2% of the total measured  $^{14}\text{C}$  atoms for typical CRONUS-A aliquots (3–4 g of quartz). Excluding one outlier ( $> 3\sigma$  deviation from the mean), the measured in-situ  $^{14}\text{C}$  concentrations follow a normal distribution ( $p = 0.98$ ) with a mean value of  $7.279 (\pm 0.03) \cdot 10^5$  at/g quartz. Total carbon yields of CRONUS-A were  $4.7 (\pm 0.3) \mu\text{gC/g}$  quartz after correction for a total average blank and carrier contribution of  $17.4 \mu\text{gC}$ . CRONUS-N was measured five times and the measured  $^{14}\text{C}$  concentrations were corrected for normal distributed blank of  $1.94 (\pm 0.56) \cdot 10^4$  atoms. The blank correction is significant and represents ca. 20–30% of the total collected  $^{14}\text{C}$  concentration (for 4–6 g of quartz). From the five measurements, the first measured value (CRONUS-N-201) yielded a  $^{14}\text{C}$  concentration 200% above the following measurements along with a significantly higher carbon yield, suggesting some contamination prior or during the extraction. This outlier ( $> 3\sigma$  deviation from the mean) was excluded. The four valid blank-corrected CRONUS-N  $^{14}\text{C}$  concentrations also follow a normal distribution of  $1.24 (\pm 0.17) \cdot 10^4$  at/g quartz ( $p = 0.40$ ) and provided

a mean  $\text{CO}_2$  yield of  $4.3 (0.3) \mu\text{gC/g}$  quartz (Fig. 4).

For both materials, the in-situ  $^{14}\text{C}$  concentrations determined on the new and the previous ETH extraction systems agree within uncertainty (Fig. 5) despite the modifications in the extraction procedure outlined above. Moreover, there is a significant improvement in the reproducibility of the CRONUS-A sample with a reduction of the average variance from 5.5% to 0.4%. This improvement is attributed to an enhanced temperature control and, thus, more stable temperatures in the extraction furnace. Coupled with use of an automated extraction procedure (cf. [22]) and the addition of a  $\text{CO}_2$  carrier gas these modifications ensure uniform and consistent extraction conditions even with alternating users. Comparison of all available  $^{14}\text{C}$  data for CRONUS-A shows the large variability between individual laboratories ( $-9/+8\%$  around the mean interlaboratory value), which exceeds the typical variance within each lab ( $\sim 5\%$ ). These results correspond to observations of previous interlaboratory comparison that found an overdispersion in the in-situ  $^{14}\text{C}$  data for CRONUS-A [18]. The data from our new

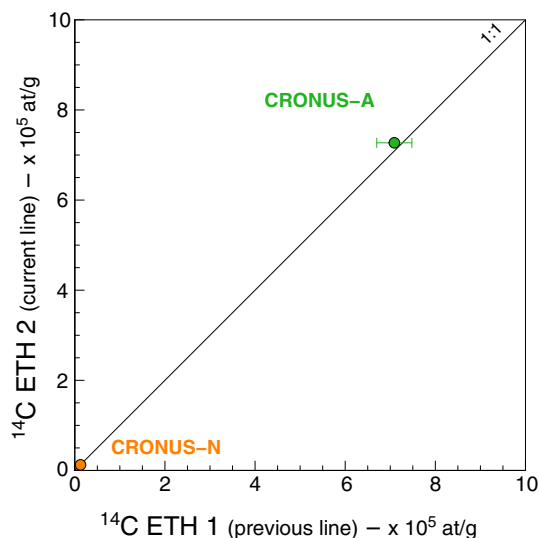


**Fig. 5.** Comparison between average concentrations of CRONUS-A and CRONUS-N measured on the new and the previous ETH extraction system [25] showing the good agreement between both systems.

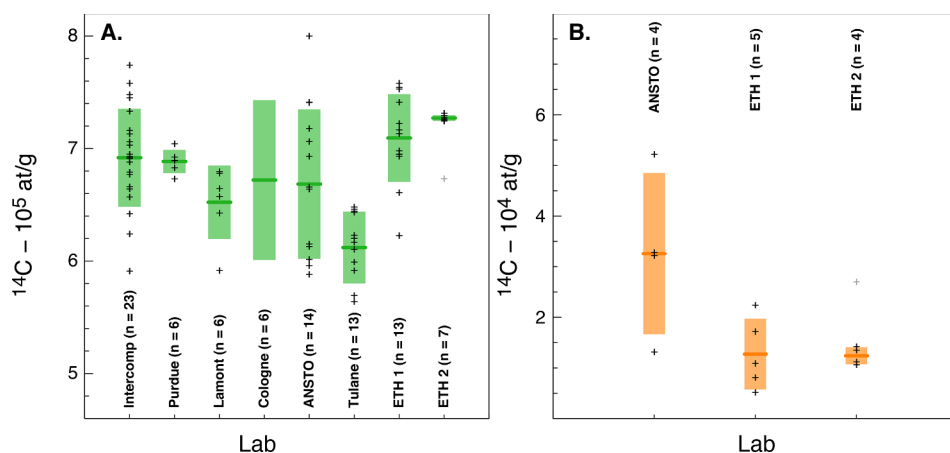


**Fig. 6.** Interlaboratory comparison including all previously reported  $^{14}\text{C}$  concentrations for CRONUS-A (A.) and CRONUS-N (B.) as well as the reported  $1\sigma$  uncertainty. Data are taken from Jull et al. [18] for the global intercomparison data, Lifton et al. [22] for Purdue, Goehring et al. [11] for Lamont, Fülöp et al. [4] for Cologne, Fülöp et al. [5] for ANSTO, Goehring et al. [8] for Tulane and Lupker et al. [25] for ETH 1 and the present study for ETH 2. Colored boxes represent mean and standard deviation of individual measurements (crosses) reported in the respective publications. Individual measurement data was not reported by Fülöp et al. [4] for Cologne.

extraction system represent the highest average  $^{14}\text{C}$  concentrations reported so far for CRONUS-A along with the lowest intralaboratory variability (see Fig. 6).

Reasons for the large interlaboratory discrepancies remain unclear and might be linked to the various analytical extraction protocols used to determine the  $^{14}\text{C}$  concentrations. Current protocols include different heating temperatures and durations, gas cleaning steps and AMS measurements procedures making direct comparison difficult. Depending on the system design, extractions are performed at lower temperatures (1100 °C) using a  $\text{LiBO}_2$  flux to dissolve the sample [22,11,8], as off-line batches at high temperature (1650 °C) but without additional  $\text{O}_2$  [4,5], or at high temperatures in the presence of  $\text{O}_2$  for both ETH systems (note that in systems using high temperatures around 1650 °C, or slightly above, quartz is not melted but sometime sintered during the extraction). In addition to variable extraction temperatures, different heating durations of 2, 3, and  $2 \times 2$  h have been reported as well as other differences in the gas cleaning protocols and the numbers and/or order of cryogenic traps. Finally, the AMS measurement of the  $^{14}\text{C}/^{12}\text{C}$  ratio from the extracted  $\text{CO}_2$  is either performed after graphitization of the sample [22,11,5] or directly on  $\text{CO}_2$  using a gas source AMS [15,5] and this study. The number of laboratories reporting  $^{14}\text{C}$  concentrations for CRONUS-N is much lower [25,5] impeding broader comparisons. Average CRONUS-N concentrations measured here are lower than those found by Fülöp et al. [5] but agree well with the previous ETH extraction system [25] albeit with an improved variance of 14% compared to the 55%.

The reproducibility of reference in-situ  $^{14}\text{C}$  material (mainly CRONUS-A) between labs represents a major challenge that needs to be overcome in order to further develop the use of in-situ  $^{14}\text{C}$  as a reliable addition to other cosmogenic nuclides. Understanding the underlying reasons for the large lab-to-lab variability therefore requires a continuing effort to compare and exchange data, reference material and measurement protocols.

#### 4. Conclusions

The extraction system described in this contribution was designed based on the experience gained with the previous system at ETH (routinely used until 2016, [14,15,25]) in order to advance in-situ  $^{14}\text{C}$  extraction procedures and improve overall reliability of in-situ  $^{14}\text{C}$  analyses. Automation of the main analytical steps resulted in a marked decrease in the required attendance time of the line operator. The samples are loaded manually into the furnace but the system runs autonomously through the time-consuming  $\text{CO}_2$  extraction and most of the sample cleaning procedures. The manual gas cleaning steps have been significantly simplified and reduced to only one cryogenic trap. The use of He gas allows efficient line flushing (cleaning) and gas transport, a major advantage compared to an entirely high vacuum

system that requires long pumping down times to reach pressures of  $10^5$ – $10^{-8}$  mbar.

Thanks to its excellent performance, low maintenance and very good data reproducibility, the new in-situ  $^{14}\text{C}$  extraction line is now routinely used to analyze natural quartz samples. Further developments and tests are nevertheless planned in the near future to improve the accuracy and precision of the method. These tests target the questions of: i) the exact sources of the system blanks to further decrease background blank levels, ii) the role of heating temperature and duration to ensure all in-situ  $^{14}\text{C}$  is quantitatively extracted from the samples, iii) the purity of the gases produced after the extraction and purification steps, iv) the use of larger quartz samples compared to present ( $> 6$  g) to increase signal to blank ratios of low in-situ  $^{14}\text{C}$  concentration samples, and v) the increase of the sample throughput of the line.

#### Declaration of Competing Interest

The authors declare that they have no known competing financial interests or personal relationships that could have appeared to influence the work reported in this paper.

#### Acknowledgments

The construction of a new extraction system was made possible through funding by the ETH Scientific Equipment Program and contributions from the Department of Earth Sciences at ETH as well as from several professorships in the Earth Science and Physics departments. The authors thank R. Wieler, S. Ivy-Ochs and H. Busemann for discussions of the new developments. A. Süsli, R. Gruber, P. Vogel and S. Bühlmann are thanked for their help with the construction. T. Jull is thanked for preparing and sharing the CRONUS reference quartz. N. Lifton is thanked for his constructive review and I. Vickridge for the efficient editorial handling of the manuscript.

#### References

- [1] R.K. Anderson, G.H. Miller, J.P. Briner, N.A. Lifton, S.B. DeVogel, A millennial perspective on Arctic warming from  $^{14}\text{C}$  in quartz and plants emerging from beneath ice caps, *Geophys. Res. Lett.* 35 (2008) L01502, <https://doi.org/10.1029/2007GL032057>.
- [2] T.J. Dunai, *Cosmogenic Nuclides: Principles Concepts and Applications in the Earth Surface Sciences*, 2010, pp. 1–199.
- [3] C.J. Fogwill, C.S.M. Turney, N.R. Golledge, D.H. Rood, K. Hippe, L. Wacker, R. Wieler, E.B. Rainsley, R.S. Jones, Drivers of abrupt Holocene shifts in West Antarctic ice stream direction determined from combined ice sheet modelling and geologic signatures, *Antarctic Sci.* 26 (2014) 674–686, <https://doi.org/10.1017/S0954102014000613>.
- [4] R.-H. Fülöp, P. Bishop, D. Fabel, G.T. Cook, J. Everest, C. Schnabel, A.T. Codilean, S. Xu, Quantifying soil loss with in-situ cosmogenic  $^{10}\text{Be}$  and  $^{14}\text{C}$  depth-profiles, *Quat. Geochronol.* 27 (2015) 78–93, <https://doi.org/10.1016/j.quageo.2015.01.003>.
- [5] R.-H. Fülöp, D. Fink, Bin Yang, A.T. Codilean, A. Smith, L. Wacker, V. Levchenko,

- T.J. Dunai, The ANSTO – university of Wollongong in-situ<sup>14</sup>C extraction laboratory, Nuclear Inst. Meth. Phys. Res. B 1–0 (2018), <https://doi.org/10.1016/j.nimb.2018.04.018>.
- [6] R.H. Fülöp, P. Naysmith, G.T. Cook, D. Fabel, S. Xu, P. Bishop, azu\_js\_rc 52, Update on the Performance of the SUERC In Situ Cosmogenic <sup>14</sup>C Extraction Line, 2010, pp. 1288–1294, <https://doi.org/10.1017/S0033822200046373>.
- [7] R.H. Fülöp, L. Wacker, T.J. Dunai, Progress report on a novel in situ <sup>14</sup>C extraction scheme at the University of Cologne, Nucl. Instrum. Meth. Phys. Res., Sect. B 361 (2015) 20–24, <https://doi.org/10.1016/j.nimb.2015.02.023>.
- [8] B.M. Goehring, J. Wilson, K. Nichols, A fully automated system for the extraction of in situ cosmogenic carbon-14 in the Tulane University cosmogenic nuclide laboratory, Nucl. Inst. Meth. Phys. Res. B 455 (2019) 284–292, <https://doi.org/10.1016/j.nimb.2019.02.006>.
- [9] B.M. Goehring, P. Muzikar, N.A. Lifton, An in situ <sup>14</sup>C–<sup>10</sup>Be Bayesian isochron approach for interpreting complex glacial histories, Quat. Geochronol. 15 (2013) 61–66, <https://doi.org/10.1016/j.quageo.2012.11.007>.
- [10] B.M. Goehring, J.M. Schaefer, C. Schluechter, N.A. Lifton, R.C. Finkel, A.J.T. Jull, N. Akcar, R.B. Alley, The Rhone Glacier was smaller than today for most of the Holocene, Geology 39 (2011) 679–682, <https://doi.org/10.1130/G32145.1>.
- [11] B.M. Goehring, I. Schimmelpfennig, J.M. Schaefer, Capabilities of the Lamont-Doherty earth observatory in situ <sup>14</sup>C extraction laboratory updated, Quat. Geochronol. 19 (2014) 194–197, <https://doi.org/10.1016/j.quageo.2013.01.004>.
- [12] K. Hippe, Constraining processes of landscape change with combined in situ cosmogenic <sup>14</sup>C–<sup>10</sup>Be analysis, Quat. Sci. Rev. 173 (2017) 1–19, <https://doi.org/10.1016/j.quascirev.2017.07.020>.
- [13] K. Hippe, S. Ivy-Ochs, F. Kober, J. Zasadni, R. Wieler, L. Wacker, P.W. Kubik, C. Schlüchter, Chronology of Lateglacial ice flow reorganization and deglaciation in the Gotthard Pass area, Central Swiss Alps, based on cosmogenic <sup>10</sup>Be and in situ <sup>14</sup>C, Quat. Geochronol. 19 (2014) 14–26, <https://doi.org/10.1016/j.quageo.2013.03.003>.
- [14] K. Hippe, F. Kober, H. Baur, M. Ruff, L. Wacker, R. Wieler, The current performance of the in situ <sup>14</sup>C extraction line at ETH, Quat. Geochronol. 4 (2009) 493–500, <https://doi.org/10.1016/j.quageo.2009.06.001>.
- [15] K. Hippe, F. Kober, L. Wacker, S.M. Fahrni, S. Ivy-Ochs, N. Akcar, C. Schlüchter, R. Wieler, An update on in situ cosmogenic <sup>14</sup>C analysis at ETH Zürich, Nucl. Instrum. Meth. Phys. Res., Sect. B 294 (2013) 81–86, <https://doi.org/10.1016/j.nimb.2012.06.020>.
- [16] K. Hippe, F. Kober, G. Zeilinger, S. Ivy-Ochs, C. Maden, L. Wacker, P.W. Kubik, R. Wieler, Quantifying denudation rates and sediment storage on the eastern Altiplano, Bolivia, using cosmogenic <sup>10</sup>Be, <sup>26</sup>Al, and in situ <sup>14</sup>C, Geomorphology 179 (2012) 58–70, <https://doi.org/10.1016/j.geomorph.2012.07.031>.
- [17] K. Hippe, N.A. Lifton, azu\_js\_rc 56, Calculating Isotope Ratios and Nuclide Concentrations for In Situ Cosmogenic <sup>14</sup>C Analyses, 2014, pp. 1167–1174, <https://doi.org/10.2458/56.17917>.
- [18] A.J.T. Jull, E.M. Scott, P. Bierman, The CRONUS-Earth inter-comparison for cosmogenic isotope analysis, Quat. Geochronol. 26 (2015) 3–10, <https://doi.org/10.1016/j.quageo.2013.09.003>.
- [19] F. Kober, K. Hippe, B. Salcher, R. Grischott, R. Zurfluh, I. Hajdas, L. Wacker, M. Christl, S. Ivy-Ochs, Postglacial to Holocene landscape evolution and process rates in steep alpine catchments, Earth Surf. Process. Landforms 74 (2018) 5–17, <https://doi.org/10.1002/esp.4491>.
- [20] F. Kober, K. Hippe, B. Salcher, S. Ivy-Ochs, P.W. Kubik, L. Wacker, N. Hahnen, Debris-flow-dependent variation of cosmogenically derived catchment-wide denudation rates, Geology 40 (2012) 935–938, <https://doi.org/10.1130/G33406.1>.
- [21] D. Lal, Cosmic ray labeling of erosion surfaces: in situ nuclide production rates and erosion models, Earth Planet. Sci. Lett. 104 (1991) 424–439, [https://doi.org/10.1016/0012-821X\(91\)90220-C](https://doi.org/10.1016/0012-821X(91)90220-C).
- [22] N. Lifton, M. Caffee, R. Finkel, S. Marrero, K. Nishiizumi, F.M. Phillips, B. Goehring, J. Gosse, J. Stone, J. Schaefer, B. Theriault, A.J.T. Jull, K. Fifield, In situ cosmogenic nuclide production rate calibration for the CRONUS-Earth project from Lake Bonneville, Utah, shoreline features, Quat. Geochronol. 26 (2015) 56–69, <https://doi.org/10.1016/j.quageo.2014.11.002>.
- [23] N. Lifton, B. Goehring, J. Wilson, T. Kubley, M. Caffee, Progress in automated extraction and purification of in situ <sup>14</sup>C from quartz: results from the Purdue in situ <sup>14</sup>C laboratory, Nucl. Instrum. Meth. Phys. Res. Sect. B 361 (2015) 381–386, <https://doi.org/10.1016/j.nimb.2015.03.028>.
- [24] N.A. Lifton, A. Jull, J. Quade, A new extraction technique and production rate estimate for in situ cosmogenic <sup>14</sup>C in quartz, Geochim. Cosmochim. Acta 65 (2001) 1953–1969, [https://doi.org/10.1016/s0016-7037\(01\)00566-x](https://doi.org/10.1016/s0016-7037(01)00566-x).
- [25] M. Lupker, K. Hippe, L. Wacker, F. Kober, C. Maden, R. Braucher, D. Bourlès, J.R.V. Romani, R. Wieler, Depth-dependence of the production rate of in situ <sup>14</sup>C in quartz from the Leymon High core, Spain, Quat. Geochronol. 28 (2015) 80–87, <https://doi.org/10.1016/j.quageo.2015.04.004>.
- [26] G.H. Miller, J.P. Briner, N.A. Lifton, R.C. Finkel, Limited ice-sheet erosion and complex exposure histories derived from in situ cosmogenic <sup>10</sup>Be, <sup>26</sup>Al, and <sup>14</sup>C on Baffin Island, Arctic Canada, Quat. Geochronol. 1 (2006) 74–85, <https://doi.org/10.1016/j.quageo.2006.06.011>.
- [27] S.M. Mudd, Detection of transience in eroding landscapes, Earth Surf. Process. Landforms 42 (2016) 24–41, <https://doi.org/10.1002/esp.3923>.
- [28] I. Schimmelpfennig, J.M. Schaefer, B.M. Goehring, N. Lifton, A.E. Putnam, D.J.A. Barrell, Calibration of the in situ cosmogenic <sup>14</sup>C production rate in New Zealand's Southern Alps, J. Quatern. Sci. 27 (2012) 671–674, <https://doi.org/10.1002/jqs.2566>.
- [29] H.-A. Synal, M. Stocker, M. Suter, MICADAS: a new compact radiocarbon AMS system, Nucl. Instrum. Meth. Phys. Res., Sect. B 259 (2007) 7–13, <https://doi.org/10.1016/j.nimb.2007.01.138>.
- [30] L. Tyroller, M.S. Brennwald, H. Busemann, C. Maden, H. Baur, R. Kipfer, Negligible fractionation of Kr and Xe isotopes by molecular diffusion in water, Earth Planet. Sci. Lett. 492 (2018) 73–78, <https://doi.org/10.1016/j.epsl.2018.03.047>.
- [31] L. Wacker, S.M. Fahrni, I. Hajdas, M. Molnar, H.A. Synal, S. Szidat, Y.L. Zhang, A versatile gas interface for routine radiocarbon analysis with a gas ion source, Nucl. Inst. Meth. Phys. Res. B 294 (2013) 315–319, <https://doi.org/10.1016/j.nimb.2012.02.009>.
- [32] D. White, R.-H. Fülöp, P. Bishop, A. Mackintosh, G. Cook, Can in-situ cosmogenic <sup>14</sup>C be used to assess the influence of clast recycling on exposure dating of ice retreat in Antarctica? Quat. Geochronol. 6 (2011) 289–294, <https://doi.org/10.1016/j.quageo.2011.03.004>.
- [33] C. Wirsig, S. Ivy-Ochs, N. Akçar, M. Lupker, K. Hippe, L. Wacker, C. Vockenhuber, C. Schlüchter, Combined cosmogenic <sup>10</sup>Be, in situ <sup>14</sup>C and <sup>36</sup>Cl concentrations constrain Holocene history and erosion depth of Gruben glacier (CH), Swiss J. Geosci. 1–10 (2016), <https://doi.org/10.1007/s00015-016-0227-2>.
- [34] N.E. Young, J.M. Schaefer, B. Goehring, N. Lifton, I. Schimmelpfennig, J.P. Briner, West Greenland and global in situ<sup>14</sup>C production-rate calibrations, J. Quatern. Sci. 29 (2014) 401–406, <https://doi.org/10.1002/jqs.2717>.